

- <sup>26</sup>T. Madey and J. T. Yates, Jr., *Surface Sci.* **11**, 327 (1968).
- <sup>27</sup>M. Nishijima and F. M. Propst, *J. Vacuum Sci. Technol.* **7**, 420 (1970).
- <sup>28</sup>M. Nishijima and F. M. Propst, *J. Vacuum Sci. Technol.* **7**, 410 (1970).
- <sup>29</sup>J. A. Becker, E. J. Becker, and R. G. Brandes, *J. Appl. Phys.* **32**, 411 (1961).
- <sup>30</sup>V. S. Fomenko, in *Handbook of Thermionic Properties*, edited by G. V. Samsonov,
- <sup>31</sup>R. V. Culver and F. C. Tompkins, in *Advances in Catalysis*, edited by D. D. Eley, P. W. Selwood, and P. B. Weisz (Academic, New York, 1959), Vol. 11, p. 97.
- <sup>32</sup>J. Franck, *Trans. Faraday Soc.* **21**, 536 (1926); E. U. Condon, *Phys. Rev.* **28**, 1182 (1926); **32**, 858 (1928).
- <sup>33</sup>H. D. Hagstrum, *Rev. Mod. Phys.* **23**, 185 (1951).
- <sup>34</sup>P. M. Morse, *Phys. Rev.* **34**, 57 (1929).
- <sup>35</sup>L. Pauling and E. B. Wilson, Jr., *Introduction to Quantum Mechanics with Application to Chemistry* (McGraw-Hill, New York, 1935).
- <sup>36</sup>M. Born and J. E. Mayer, *Z. Physik* **75**, 1 (1932).
- <sup>37</sup>H. D. Hagstrum, *Phys. Rev.* **96**, 336 (1954).
- <sup>38</sup>F. M. Propst and T. C. Piper, *J. Vacuum Sci. Technol.* **4**, 53 (1967).
- <sup>39</sup>F. M. Propst and E. Lüscher, *Phys. Rev.* **132**, 1037 (1963).

PHYSICAL REVIEW B

VOLUME 2, NUMBER 7

1 OCTOBER 1970

## Mössbauer Spectroscopy in Group-III Antimonides\*

R. A. Pruitt† and S. W. Marshall

*Department of Physics, Colorado State University, Fort Collins, Colorado 80521*

and

C. M. O'Donnell

*Department of Chemistry, Colorado State University, Fort Collins, Colorado 80521*

(Received 16 April 1970)

Mössbauer absorption spectra of the group-III antimonides AlSb, GaSb, and InSb, and ternary alloys of the latter two compounds have been taken at 78 °K, using the 37.2-keV,  $\frac{7}{2}^+ \rightarrow \frac{5}{2}^+$  transition in  $\text{Sb}^{121}$ . An absorber of  $\text{KSbF}_6$  was used to help determine the nuclear factor  $\delta R/R = (-6.7 \pm 3) \times 10^{-4}$ . Chemical bonding in these compounds has both ionic and covalent character raising the question of relative ionicity. Molecular-orbital (MO) and linear-combination-of-atomic-orbital calculations, together with an assessment of electronegativity differences, predict that ionicity increases for the series GaSb, InSb, and AlSb, whereas measurements of the Mössbauer isomer shift along with some bulk and atomic properties show that ionicity increases in the series InSb, GaSb, and AlSb. Interpretation of the isomer-shift data is somewhat complicated by shielding of the  $p$  electrons at the Sb nucleus, but electron populations determined by MO calculations indicate that the  $5s$ -electron population is nearly the same on the Sb nuclei in the three compounds, in accord with the results of Hafemeister *et al.* on alkali iodides and those of Lees and Flinn on tin compounds. Thus, the  $5s$ -electron population tends to be constant in compounds of these three elements from the same row of the periodic chart. Though the single-line Mössbauer absorption spectra were broad for some absorbers, there was no evidence of quadrupole hyperfine structure which would have been apparent from asymmetry of the absorption lines.

## 1. INTRODUCTION

In the absence of hyperfine splitting, Mössbauer absorption lines unambiguously reflect the relative electron densities, measured at the nucleus, between absorbers composed of different solid materials. Since the isomer-shift  $\delta$  may be written as the product of an electronic factor and a nuclear factor, the electron densities may be measured only after the nuclear factor for a particular  $\gamma$ -ray transition has been determined. In this paper we discuss results obtained from Mössbauer

experiments using  $\gamma$  rays from the 37.2-keV,  $\frac{7}{2}^+ \rightarrow \frac{5}{2}^+$  transition in  $\text{Sb}^{121}$  which, together with calculations of electron densities arising from various configurations, have permitted determination of the nuclear factor for this transition. We have used the nuclear-factor and isomer-shift measurements on the group-III antimonides, AlSb, GaSb, and InSb, to measure the degree of ionicity in these compounds, in a manner similar to that of Hafemeister *et al.* for compounds of iodine.<sup>2</sup> The ternary alloys  $\text{Ga}_x\text{In}_{1-x}\text{Sb}$  were studied as well to see

if the average electron densities change monotonically (revealed through isomer-shift measurements) and if any significant lattice distortion occurs (seen through hyperfine splitting) as  $x$  goes from 0 to 1.

## II. BACKGROUND

The compounds studied in this investigation all have the zinc-blende (or sphalerite) structure,<sup>3</sup> which is like the diamond structure except that the group-III atoms, Al, Ga, In, and the group-V atoms, Sb, each lie on a fcc sublattice, the two sublattices displaced relative to each other by one-quarter of the length of the body diagonal of the cube.

Each of the group-III atoms, when free, has three valence electrons in an  $s^2p$  configuration, while each antimony possesses five valence electrons nominally in an  $s^2p^3$  configuration. In chemical combination, there exist several possible charge distributions for the ions. Each of the group-III atoms may lose its three valence electrons to the antimony resulting in a net charge of +3 on the group-III ions and a -3 on the antimony, forming an ionic bond. In general, this distribution is written as  $A^{+3}B^{-3}$ .<sup>4</sup> Another possibility is for Sb to donate electrons to the group-III atoms with the result that electron-pair bonds are formed between the two ion types. In an idealized case, the bond would be characterized by an  $sp^3$  configuration and the group-III ions would have, on the average, a net charge of -1. This type of bond is described<sup>4</sup> as a covalent bond and the compound could be denoted by  $A^{-1}B^{+1}$ .

Referring to previous definitions of covalency and ionicity, compounds are neither completely ionic nor completely covalent, falling somewhere between these two extreme cases. Many investigators, therefore, have worked on schemes and methods of determination of the fractional ionicity of the bonds in these compounds. Some 35 years ago Pauling<sup>5</sup> developed a definition of the fractional ionic character  $F(A,B)$  of the bond between elements  $A$  and  $B$ . According to his definition

$$F(A,B) = 1 - \exp\left[-\frac{1}{4}(X_A - X_B)^2\right], \quad (1)$$

where  $X_A$  and  $X_B$  are the electronegativities for elements  $A$  and  $B$  determined from heats of formation of diatomic compounds. Although it has proved difficult to formulate a quantitative relation between the partial ionic character of a bond and the electronegativity differences  $\Delta X = |X_A - X_B|$ , ionic character generally increases as  $\Delta X$  between the two members of the bond increases.<sup>6</sup>

In the case that each of the group-III antimonides has basically the same type of bond and that

all have a common Sb anion, electronegativity differences may indicate the fractional ionic character of the bonds. In Table I we see that the electronegativity differences between gallium and antimony are less than the electronegativity differences between indium and antimony, so that, on this basis, it would be expected that GaSb would be *less* ionic than InSb and that AlSb would be the *most* ionic of the three compounds. Pauling has also stated a principle of *electroneutrality* for the intermetallic compounds which states that "in general the electronic structure of substances is such as to cause each atom to have essentially zero resultant charge,"<sup>7</sup> that is, in the range -1 to +1. As will be shown, all results, both experimental and calculational, presented herein are in agreement with this principle of electroneutrality.

Coulson *et al.*<sup>8</sup> have calculated the net charges on the ions in III-V compounds by means of a linear-combination-of-atomic-orbital-molecular-orbital (LCAO-MO) method. They view the ionic-covalent bonding of the two nearest-neighbors group-III atoms and group-V atoms, as a combination of  $sp^3$ -hybrid wave functions:

$$\psi = \lambda \Phi_{III} + \Phi_V, \quad (2)$$

where  $\lambda$  is a variational parameter used to determine the net charge of the two atoms. Coulson's results for the group-III antimonides (see Table I) indicate that these compounds do not form neutral bonds and are somewhat ionic. Furthermore, Coulson concludes that GaSb is the least ionic (consistent with the definitions of ionic and covalent, above) of the three compounds, in agreement with the predictions of electronegativity differences. But Coulson's LCAO calculations and electronegativity differences disagree concerning the ionicity of InSb and AlSb.

Phillips and Van Vechten<sup>9</sup> have recently defined an *absolute* scale of fractional ionicity  $f_i$  based on the ionic and covalent energy gaps  $C$  and  $E_h$ , re-

TABLE I. Charge considerations in some group-III antimonides.

	AlSb	GaSb	InSb
Electronegativity differences (Ref. 5)	0.44	0.24	0.27
Net charge on Sb (Coulson) (Ref. 8)	-0.44	-0.43	-0.46
Fractional ionic character (Ref. 9)	0.44	0.26	0.32
Net charge on Sb <sup>a</sup>	0.38	0.59	0.43
<i>s</i> -electron population <sup>a</sup>	1.68	1.67	1.71
<i>p</i> -electron population <sup>a</sup>	2.94	2.75	2.86
Overlap <sup>a</sup>	0.51	0.52	0.49

<sup>a</sup>This paper.

spectively, defined in terms of the electronic dielectric constant. Values for  $f_i$  for the group-III antimonides are presented in Table I where  $f_i$  is 0.00 for a covalent compound and 1.00 for an ionic compound. These values are seen to give the same ordering of the compounds as that given by the electronegativity differences, namely, ionicity increases from GaSb to InSb to AlSb.

In addition to Mössbauer effect measurements, the techniques and results of which will be discussed in the following sections, we have made extended Hückel MO computations<sup>10</sup> for these antimonides. Here MO are formed from a linear combination of Slater-type atomic orbitals (STO's). The functional form of the STO is

$$\psi = N r^{(n^*-1)} e^{(-Z-\sigma)r/n^*} a_0 Y(l, m | \theta, \phi), \quad (3)$$

where  $N$  is the normalization factor,  $r$  is the distance from the center of the atom,  $n^*$  is the effective principal quantum number,  $Z$  is the atomic number,  $\sigma$  is the Slater shielding coefficient,  $a_0$  is the Bohr radius, and  $Y(l, m | \theta, \phi)$  is the spherical harmonic which controls the symmetry of the orbital. In the region of chemical binding, a single STO can be made to give reasonable agreement with a self-consistent-field Hartree-Fock wave function by carefully choosing the orbital exponent  $(Z - \sigma)/n^*$ , commonly referred to as "Zed." In our work we used the single Zed values determined by Clementi *et al.*<sup>11</sup> for each ion type and the actual principal quantum number for each ion type in the compounds considered. The Coulomb integrals  $H_{ii}$  for the program are taken from the nonrelativistic Hartree-Fock-Slater energy levels  $E_{nl}$  given by Herman and Skillman.<sup>12</sup>

In the MO calculation we chose a molecule of 17 ions consisting of a central Sb surrounded by its four nearest-neighbor group-III ions, each of which is also surrounded by its four nearest-neighbor Sb ions (one of which is the central Sb). Values for both the electronic populations and the overlaps given in Table I are those obtained for the central Sb ion. Coordinates for each of the 17 atoms involved in each of the computations were determined from the lattice constants obtained by Giesecke and Pfister.<sup>13</sup>

Both Löwdin<sup>14</sup> and Mulliken<sup>15</sup> population analyses were made to obtain measures of the net charge on the Sb ions. But Löwdin<sup>14</sup> has pointed out that because of the properties of the basis functions used, these values do not necessarily give the actual physical charges on the ions. Although the results of the two methods do not agree numerically, there is general agreement in the order of the charge variation from compound to compound. The Mulliken values along with their corresponding antimony 5s and

5p electron populations appear in Table I because the overlap values also given in the same table are based upon the Mulliken analysis. From the population analyses for AlSb and GaSb we see a much larger fluctuation in the  $p$ -electron population in these two compounds than in the  $s$ -electron population. Since computations were carried out on all three compounds in the same way, the results for InSb which are contrary to those for AlSb and GaSb must be suspect. It should be pointed out that inclusion of further parametrization, such as correction for neighboring atom potentials, would not effect this ordering.

### III. EXPERIMENTAL TECHNIQUES

The 100- $\mu$ Ci source of 37.2-keV Mössbauer  $\gamma$  rays was obtained commercially in the chemical form of BaSnO<sub>3</sub>.<sup>16</sup> Absorber materials were obtained from numerous sources.<sup>17</sup> The material in each of the absorbers was powdered and contained approximately 6 mg/cm<sup>2</sup> of natural antimony mixed with powdered Lucite. The mixtures were in turn compressed in a heated press and formed into disks 0.3 cm thick by 2.54 cm diam.

A standard transmission geometry was used with the source and absorber mounted in the exchange-gas chamber of a cryostat.<sup>18</sup> All measurements were made with both the source and absorber at 78 °K. The source was moved by a thin-walled stainless-steel tube driven by an electromechanical transducer built from plans furnished by the National Bureau of Standards.<sup>19</sup> The driving voltage was derived from the analog signal of a 400-channel analyzer operating in a crystal-controlled multi-scaling mode to impart to the source a constant acceleration. The spectrometer was velocity calibrated by using a source of Co<sup>57</sup> in palladium and an iron foil absorber. Details of the velocity calibration appear elsewhere.<sup>20</sup>

The  $\gamma$  rays passing through the absorber were allowed to exit the Dewar through two 10-mil Be windows. The  $\gamma$ -ray spectrum was then detected with a proportional counter filled with a mixture of xenon and methane gas at 2 atm. A 10-mil exit window in the counter helped prevent scattering of radiation from the internal walls of the detector. Because the 37.2-keV  $\gamma$  rays exceeded the energy necessary to eject a  $K$  electron from a xenon atom, there appeared an escape peak (see Fig. 1) whose energy of 7.5 keV was determined by

$$E_{e.p.} = E_i - E_f, \quad (4)$$

where  $E_i = 37.2$  keV is the incident energy of the  $\gamma$  rays and  $E_f$  is (in this case) the  $K$ -emission edge energy for xenon which is 29.7 keV.<sup>21</sup> The high probability of ejecting a  $K$  electron combined with the detector's higher counting efficiency for the low-

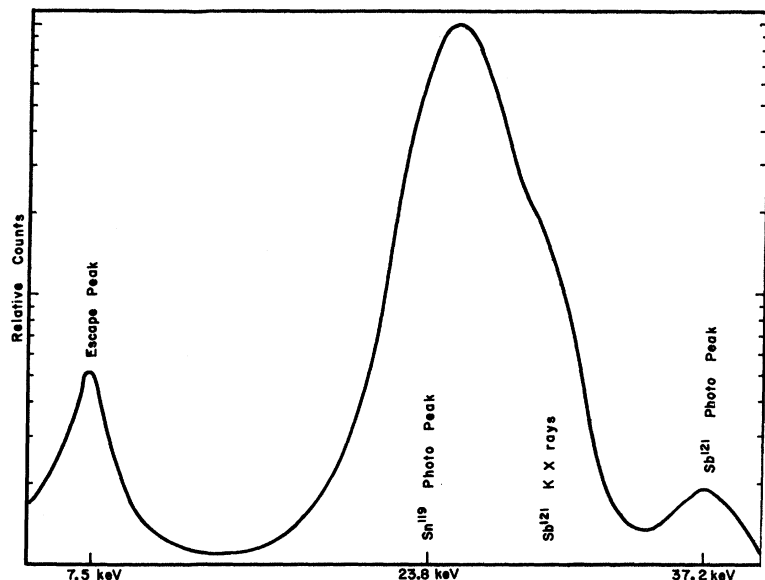


FIG. 1. Typical pulse-height-analyzer spectrum for  $\text{Sn}^{121}$  source.

energy process resulted in an escape peak somewhat larger than the 37.2-keV photopeak. By setting the analyzer's single-channel window on the escape peak, the counting rate was enhanced.

Since the counting rate in the single-channel window was approximately 30 counts/sec, a period of over four days was required for each absorber to accumulate a single 200-channel spectrum. During this period, data were collected and the velocity was checked every 12 h. All 12-h accumulations were individually analyzed, and those that showed no inconsistencies were added together.

#### IV. THEORETICAL CONSIDERATIONS

There are several ways in which electrons in a solid interact with the nuclei to perturb the nuclear energy levels. Of these interactions only the nuclear electric monopole and nuclear electric quadrupole interactions were considered in this investigation. Electric monopole effects displace the nuclear energy levels through electrostatic interactions of the nucleus with its surrounding electron-charge cloud.<sup>22</sup> A degeneracy may be partially removed through the interaction between the nuclear electric quadrupole moment and the electric field gradient (EFG) at the site of the nucleus produced by all charges exterior to the nucleus.<sup>23</sup>

If the source and absorber nuclei are in different chemical environments, there will, in general, be a difference between their electric monopole interactions giving rise to an energy shift in the centroid of the Mössbauer spectrum. This isomer shift as given by Shirley<sup>24</sup> is

$$\delta = F(Z)S'(Z) [ |\psi_a(0)|^2 - |\psi_s(0)|^2 ] \delta R/R, \quad (5)$$

where  $R$  is the average of the ground- and the excited-state nuclear radii,  $|\psi_a(0)|^2$  and  $|\psi_s(0)|^2$  are the nonrelativistic electronic charge densities at the absorber nuclei and source nuclei, respectively,  $\delta R$  is the difference in the excited- and the ground-state nuclear radii, and  $S'(Z)$  is a dimensionless factor to account for distortion of the electron wave functions by the nucleus and for their nonrelativistic value. Using  $R = 1.20 \times 10^{-13} A^{1/3}$ , Shirley has calculated and tabulated  $S'(Z)$ ; for antimony ( $Z = 51$ ),  $S'(Z) = 2.38$ . The factor  $F(Z)$  is

$$F(Z) = 4\pi cZe^2R^2/5E_\gamma, \quad (6)$$

and is equal to  $(3.670 \times 10^2 \text{ mm/sec}) a_0^3$  for antimony, in terms of the Bohr radius  $a_0$ .

The values of  $|\psi(0)|^2$  used herein are given in Table II and were obtained by Wilson of the Argonne National Laboratory using a Hartree-Fock self-consistent-field computation.<sup>25</sup> For an isolated antimony atom, the electronic configuration is  $\text{Kr } 4d^{10} - 5s^2 5p^3$ , and the contribution of the core electrons ( $\text{Kr } 4d^{10}$ ) is given in Table II by  $K = 93\,291$ . Compared to the isomer-shift difference obtained from configurations in Table II, second-order effects are small.

Since the isomer shift actually measures the  $s$ -electron density at the nucleus, a WWJ plot<sup>26</sup> of the total  $s$ -electrons density  $|\psi(0)|^2/a_0^3$  as a function of  $5s$ -electron character for various configurations of  $5p$ -electrons clearly shows how the total  $s$ -electron density at the nucleus varies with the addition of  $s$  and  $p$  electrons.<sup>25</sup> The results show that addition of  $s$ -electrons increases  $|\psi(0)|^2/a_0^3$ , while the addition of  $p$  electrons decreases because of shielding.

TABLE II. Values of the electron density at the nucleus for different electronic configurations of antimony (from Ref. 25).

Electron configuration	$[\psi^2(0)/a_0^3] - K$
$5s^25p^3$	27.72
$5s^25p^2$	36.22
$5s^25p^1$	40.55
$5s^25p^0$	44.45
$5s^15p^3$	18.28
$5s^15p^2$	19.97
$5s^15p^1$	22.10
$5s^15p^0$	24.59
$5s^05p^3$	00.00
$5s^05p^2$	-0.57 <sup>a</sup>
$5s^05p^1$	-0.91 <sup>a</sup>
$5s^05p^0$	-1.04 <sup>a</sup>

<sup>a</sup>Determined by extrapolation.

## V. ANALYSIS AND RESULTS

From the electronically measured half-life<sup>27</sup> of the first excited level of  $\text{Sb}^{121}$ , the narrowest possible experimental linewidth is  $2\Gamma = 2.1 \pm 0.12$  mm/sec. Using the method of Margulies and Ehrman<sup>28</sup> to account for spectral line broadening due to finite absorber thickness, we determined an effective thickness  $T_a$  yielding an apparent width,  $2\Gamma_a = 2.4 \pm 0.1$  mm/sec.  $2\Gamma_a$  was observed in the  $\text{Ga}_{0.17}\text{In}_{0.83}\text{Sb}$  absorber having a measured linewidth of  $2.39 \pm 0.12$  mm/sec (see Fig. 2). Most of the linewidths for the absorbers in this investigation were considerably larger, so that these spectra were analyzed for possible unresolved quadrupolar splitting.

The computer program<sup>29</sup> which was used to make least-squares fits of the Mössbauer spectra was modified to incorporate the line positions for the eight lines permitted by the dipole selection rules governing the  $\frac{7}{2}^+ \rightarrow \frac{5}{2}^+$  transition of  $\text{Sb}^{121}$ .<sup>30</sup> Relative intensities for the eight lines resulting from  $\frac{5}{2}^+$  to  $\frac{7}{2}^+$  dipole transitions in the absorber were determined from the squares of the appropriate Clebsch-Gordan coefficients and were expressed as constraints in the program. In searching for optimal values of the five least-squares parameters of baseline (the off-resonance counting rate), linewidth, quadrupole splitting ( $e^2qQc/4E_\gamma$ ), isomer shift, and fractional absorption (uncorrected for background), the program depends on the investigator's ability to give reasonable estimates of these parameters, which are then refined by successive iterations. With the program dependent upon the bias of the investigator the initial parameters have to be chosen with some care. Therefore, if the absorption line is broad, the investigator might assume an unresolved splitting when in reality none exists. For example, an initial estimate of a positive quadrupole splitting

parameter was made for a GaSb spectrum and the computer calculation yielded a value of  $0.60 \pm 0.30$  mm/sec. The computer result for the same data using a negative starting value for the quadrupole splitting was  $-0.60 \pm 0.26$  mm/sec. Since the quadrupole interaction in  $\text{Sb}^{121}$  results in spectral lines that are asymmetric about the isomer shift, the combination of these two calculations indicate that, within the uncertainty of the measurement, the broad Mössbauer line of this particular absorber is symmetric and is not due to unresolved hyperfine structure. As a result of the same test on other spectra, single-line computer fits of the spectra appeared satisfactory, so that the parameters were reduced to simply baseline, linewidth, isomer shift, and fractional absorption. From results of different runs on the same absorber taken several months apart we deduced that linewidths in excess of 2.4 mm/sec are traceable to slight changes in the electronics of the spectrometer because of fluctuations in the ambient temperature in the laboratory over a four-day counting period.

As can be seen in Table III the ordering according to increasing negative value of the isomer shift for the pure compounds is: AlSb, GaSb, InSb. The same general trend is seen in the isomer shifts of the alloy samples when proceeding from the alloys containing the greatest percentage of gallium to pure InSb. In order to determine the variation of charge density with isomer shift, the nuclear factor  $\delta R/R$  must be known. Accordingly, we measured the isomer shift of  $\text{KSbF}_6$  (potassium hexafluoroantimonate) given in Table III. By making extended Huckel MO calculations<sup>9</sup> on  $\text{KSbF}_6$  we find the antimony in this compound has a configuration which is nearly  $5s^0p^2$ .

Evidence from the physical properties of the group-III antimonides (see Table IV) suggests an ionicity ordering in the series AlSb, GaSb, InSb. Assuming that the bond strength decreases with decreasing

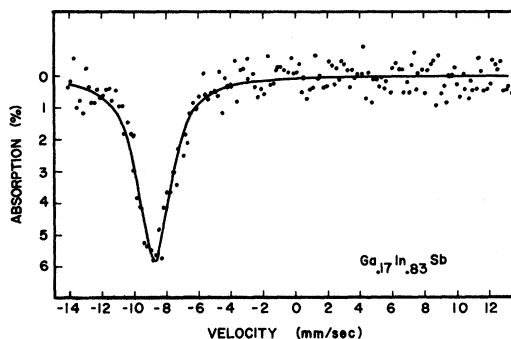


FIG. 2. Mössbauer spectrum of  $\text{Ga}_{0.17}\text{In}_{0.83}\text{Sb}$  at 78 °K. The single-line fit has a width  $2.39 \pm 0.12$  mm/sec.

TABLE III. Results of Mössbauer isomer-shift measurements on III antimonides, and ternary alloys of the composition  $\text{Ga}_x\text{In}_{1-x}\text{Sb}$ . Uncertainties given represent one standard deviation.

Compound	Isomer shift (mm/sec)
InSb	$-8.70 \pm 0.07$
$x = 0.17$	$-8.70 \pm 0.04$
$x = 0.34$	$-8.53 \pm 0.07$
$x = 0.56$	$-8.42 \pm 0.07$
$x = 0.60$	$-8.48 \pm 0.18$
$x = 0.80$	$-8.49 \pm 0.05$
GaSb	$-8.35 \pm 0.05$
AlSb	$-7.79 \pm 0.06$
$\text{KSbF}_6$	$+2.52 \pm 0.20$

ionicity for the group-III antimonides, then the low melting point and the low Debye temperature of InSb would indicate that it is the most covalent of these compounds. The heats of formation also imply that InSb is again the least ionic of the compounds in Table IV. As a final argument we consider the mobilities of the charge carriers. The mobilities are affected by the ionicity of the bonds in two ways.<sup>31</sup> First, an increase in ionicity causes an increase in ion scattering, resulting in a decrease in the mobility of the carriers. Second, an increase in ionicity causes an increase in the effective masses of the charge carriers, which also results in a decrease in the carrier mobility. Applied to electron mobilities, this argument is consistent with the fact that InSb is the most covalent whereas AlSb is the most ionic of the group-III antimonides; the hole mobilities, however, do not show such a trend.

Having established from the above physical properties that InSb is the most covalent and hence has the most representative  $sp^3$  configuration of the three group-III antimonides, we can now proceed to calculate  $\delta R/R$ . Selecting charge densities from Table II for the  $5s^0p^2$  and  $5s^1p^3$  configurations and the respective isomer shifts for  $\text{KSbF}_6$  and InSb from Table IV, we obtain with the aid of Eq. (5) a value of  $(-6.7 \pm 3) \times 10^{-4}$  for the fractional change in the nuclear radius. This value may be compared to the values of  $\delta R/R$  reported (and listed here chronologically),  $(-8.5 \pm 3) \times 10^{-4}$ ,<sup>25</sup>  $(-9.5 \pm 3) \times 10^{-4}$ ,<sup>32</sup> and  $(-7.3 \pm 0.8) \times 10^{-4}$ .<sup>33</sup> It is important to note, however, that only the sign of  $\delta R/R$  is vital to the ionicity order, not its absolute value.

## VI. CONCLUSIONS

With the exception of the nuclear factor  $\delta R/R$  and the measured isomer shift for the III-V compounds investigated herein, all other terms in Eq. (5) are

positive. It can be seen from the isomer-shift results in Table III that the charge density,  $|\psi(0)|^2/a_0^3$ , for Sb decreases in InSb, GaSb, and AlSb, in that order. As noted earlier, this could be due to either a decrease in the population of  $s$  electrons or an increase in  $p$  electrons or to both effects occurring simultaneously, proceeding through the above series of compounds. The MO calculations (see Table I) for AlSb and GaSb show that the predominant variation in electron population is in the number of  $p$  electrons, with the  $s$ -electrons population remaining relatively constant. This result of  $s$ -electron constancy has also been found by Mössbauer spectroscopy in alkali iodides<sup>2</sup> and tin compounds,<sup>34</sup> both Mössbauer isotopes coming from the same row of the periodic chart as does Sb. Assuming both the same type of behavior for InSb and that the number of  $p$  electrons increases for the group-III antimonides in order InSb to GaSb to AlSb, then the smooth decrease in  $|\psi(0)|^2/a_0^3$  observed experimentally is due to shielding by  $p$  electrons. It is important to stress here the extreme sensitivity of the Mössbauer isomer shift to small changes in charge density. Moreover, the fact that the electron density at the Sb nuclei must be greater in InSb than in GaSb may be taken as evidence that the ability of Mössbauer isomer shifts to discern charge density differences surpasses that of existing theoretical approaches.

The result that Sb ions in AlSb have more electrons (but a lower electron density at the Sb nuclei because of shielding) than those in InSb shows the former is more ionic and the latter more covalent. This same smooth variation was observed in all the physical properties of the group-III antimonides re-

TABLE IV. Physical properties of the group-III antimonides.

	InSb	GaSb	AlSb	Reference
Melting point (°C)	525	712	1054	a
Debye temp. at 80 °K	228	270	350	b
Heat of formation (kcal/g atom)	$3.5 \pm 0.1$	$5.0 \pm 0.2$	...	c
Energy gap at 300 °K, eV	0.17	0.67	1.60	a
Electron mobility at 300 °K ( $\text{cm}^2/\text{V sec}$ )	78 000	4000	200	a
Hole mobility at 300 °K ( $\text{cm}^2/\text{V sec}$ )	750	1400	420	a
Dielectric constant	16.8	13.7	10.1	a
Lattice parameter (Å)	6.48	6.20	6.14	a
Density ( $\text{gm}/\text{cm}^3$ )	5.78	5.62	4.22	a
Mössbauer isomer shift, relative to InSb at 78 °K (mm/sec)	0	$+0.35 \pm 0.09$	$+0.91 \pm 0.09$	d

<sup>a</sup>C. S. Roberts, in *Intermetallic Compounds*, edited by J. H. Westbrook (Wiley, New York, 1967), p. 571.

<sup>b</sup>P. V. Gul'yaev and A. V. Petrov, *Fiz. Tverd. Tela* **1**, 368 (1959) [*Soviet Phys. Solid State* **1**, 330 (1965)].

<sup>c</sup>W. F. Schottky and M. B. Berver, *Acta Met.* **6**, 320 (1958).

<sup>d</sup>This paper.

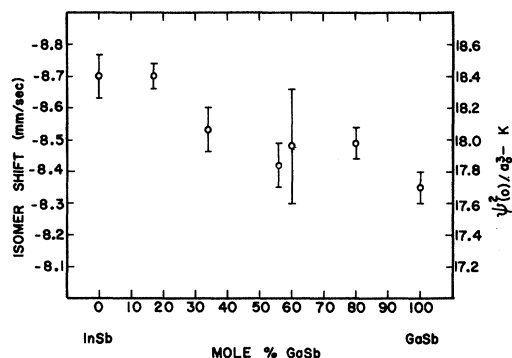


FIG. 3. Variation of isomer shift and antimony charge density (see Table IV for dimensions) with composition for the ternary alloys. The bars represent one standard deviation of uncertainty in the measurement of the isomer shift.

ported in Table IV (with the exception of hole mobilities). Furthermore, this ordering is in agreement with the results of electronegativity differences, and with Phillips's work which predicts that AlSb is the most ionic of these compounds. On the other hand, Coulson's calculated values of net charge not only

fail to show a smooth variation as we proceed down the periodic chart, but also predict that InSb rather than AlSb is the more ionic.

Finally, we note that the variation with composition of the antimony charge density in the ternary alloys is monotonic (see Fig. 3), similar to the linear variation of lattice parameter with composition (Vegard's Law) experimentally observed by Woolley and Smith.<sup>35</sup> Since the ionic contributions to the chemical bonds in GaSb and InSb are different, a regular variation of charge density in the alloys requires that the ionicity of the chemical bonds vary in a similar fashion. The unbroadened spectral line obtained using  $\text{Ga}_{0.17}\text{In}_{0.83}\text{Sb}$  absorber (Fig. 2) indicates that quadrupolar distortion is effectively nil, even though the antimony atoms in the crystal are coordinated, on the average, with two different type ions from group III. This strongly suggests that, on the average, all bonds in these alloy systems are equivalent.

#### ACKNOWLEDGMENTS

We are grateful to the University Computer Center for their assistance in helping to run Professor Cusachs's program, and we acknowledge grants from the University Faculty Improvement Committee which aided in setting up the Mössbauer laboratory.

\*This work is based upon a dissertation submitted by R. A. Pruitt in partial fulfillment of the requirements for the Ph.D. degree, Colorado State University, Fort Collins, Colo. 80521.

†Present address: Fort Hays Kansas State College, Hays, Kan. 67601.

<sup>1</sup>R. E. Snyder and G. B. Beard, *Phys. Letters* **15**, 264 (1965).

<sup>2</sup>D. W. Hafemeister, G. De Pasquali, and H. de Waard, *Phys. Rev.* **135**, B1089 (1964).

<sup>3</sup>O. Madelung, *Physics of III-V Compounds* (Wiley, New York, 1964), p. 2.

<sup>4</sup>See Ref. 3, p. 19.

<sup>5</sup>L. Pauling, *The Nature of the Chemical Bond* (Cornell U. P., Ithaca, N. Y., 1960), 3rd ed., p. 273.

<sup>6</sup>A. L. Allred, *J. Inorg. Nucl. Chem.* **17**, 215 (1961).

<sup>7</sup>L. Pauling, *J. Chem. Soc.* **1948**, 1461 (1948).

<sup>8</sup>C. A. Coulson, L. B. Reidel, and D. Stocker, *Proc. Roy. Soc. (London)* **A270**, 357 (1962).

<sup>9</sup>J. C. Phillips and J. A. Van Vechten, *Phys. Rev. Letters* **22**, 705 (1969).

<sup>10</sup>Computer program is the program Zipmol obtained from L. C. Cusachs, Tulane University, New Orleans, La.

<sup>11</sup>E. Clementi and D. L. Raimondi, *J. Chem. Phys.* **38**, 2686 (1963); E. Clementi, D. L. Raimondi, and W. P. Reinhardt, *ibid.* **47**, 1300 (1967).

<sup>12</sup>F. Herman and S. Skillman, *Atomic Structure Calculations* (Prentice-Hall, Englewood Cliffs, N. J., 1963).

<sup>13</sup>G. Giesecke and H. Pfister, *Acta Cryst.* **11**, 369 (1958).

<sup>14</sup>P. O. Löwdin, *J. Chem. Phys.* **18**, 365 (1950).

<sup>15</sup>R. S. Mulliken, *J. Chem. Phys.* **23**, 1833 (1955).

<sup>16</sup>The source was purchased from New England Nuclear Corp.

<sup>17</sup>InSb was acquired from Texas Instruments and GaSb was purchased from Bell and Howell Research Laboratories. Four of the ternary alloys were kindly furnished by J. C. Woolley of the University of Ottawa (Canada), and one was prepared at Colorado State University. A crystal of AlSb was donated by B. T. Alburn of Purdue University.

<sup>18</sup>The liquid-helium research Dewar was Model 7  $\frac{1}{2}$ " D. T. made by Janis Research Company.

<sup>19</sup>F. C. Ruegg, *Natl. Bur. Std. (U.S.) Tech. Note* **276**, 89 (1966); F. C. Ruegg and J. J. Spijkerman, *ibid.* **248**, 25 (1964).

<sup>20</sup>R. A. Pruitt, Ph.D. dissertation, Colorado State University, 1969, Appendix II (unpublished).

<sup>21</sup>M. A. Blokhin, *Methods of X-Ray Spectroscopic Research* (Pergamon, New York, 1965), p. 101 ff.

<sup>22</sup>R. L. Mössbauer and M. J. Clauser, in *Hyperfine Interactions*, edited by A. J. Freeman and R. B. Frankel (Academic, New York, 1967), p. 516.

<sup>23</sup>A. J. F. Boyle and H. E. Hall, *Rept. Progr. Phys.* **25**, 441 (1962).

<sup>24</sup>D. A. Shirley, *Rev. Mod. Phys.* **36**, 339 (1964).

<sup>25</sup>S. L. Ruby, G. M. Kalvius, G. B. Beard, and R. E.

Synder, Phys. Rev. Letters **4**, 274 (1960).

<sup>26</sup>L. R. Walker, G. K. Wertheim, and V. Jaccarino, Phys. Rev. Letters **6**, 98 (1961). Referred to as WWJ in this paper.

<sup>27</sup>Y. Y. Chu, O. C. Kistner, A. C. Li, S. Monaro, and M. L. Periman, Phys. Rev. **133**, B1361 (1964).

<sup>28</sup>S. Margulies and J. R. Ehrman, Nuclear Inst. and Methods **12**, 131 (1961).

<sup>29</sup>S. W. Marshall, J. A. Nelson, and R. M. Wilenzick, Commun. ACM **8**, 313 (1965).

<sup>30</sup>A. Abragam and F. Boutron, Compt. Rend. **252**, 2404 (1961).

<sup>31</sup>O. G. Folberth, in *Compound Semiconductors*, Vol. I, edited by R. K. Willardson and H. L. Goering (Reinhold, New York, 1961), p. 31.

<sup>32</sup>V. Kothekar, B. Z. Iofa, S. I. Semenov, and V. S. Shpinel, Zh. Eksperim. i Theor. Fiz. **55**, 160 (1968) [Soviet Phys. JETP **28**, 86 (1969)].

<sup>33</sup>S. L. Ruby and G. K. Shenoy, Phys. Rev. **186**, 326 (1969).

<sup>34</sup>J. Lees and P. A. Flinn, Phys. Letters **19**, 186 (1965).

<sup>35</sup>J. C. Woolley and B. A. Smith, Proc. Phys. Soc. (London) **72**, 214 (1958).

## Dynamic Jahn-Teller Effect in the Orbital ${}^5E$ State of $\text{Fe}^{2+}$ in CdTe

J. T. Vallin

*General Electric Research and Development Center, Schenectady, New York 12301*

(Received 26 March 1970)

A calculation of the  ${}^5E$  energy levels of  $\text{Fe}^{2+}$  in CdTe has been performed taking into account coupling between the electron system of the impurity ion and the vibrations of the host lattice. The coupling is approximated to a single pair of  $E$  modes corresponding to the  $\text{TA}(L)$  phonons. We find that even a small electron-phonon coupling not only displaces the energy levels from those of crystal-field theory, but also introduces additional transitions. We get qualitative agreement with the experimental observations for an effective spin-orbit splitting of  $20.8 \text{ cm}^{-1}$  and a Jahn-Teller energy of  $4.2 \text{ cm}^{-1}$ . We also find that we get better agreement between theory and experiment if we take spin-spin interactions into account.

### I. INTRODUCTION

Low-energy electronic levels of the  $\text{Fe}^{2+}$  ( $3d^6$ ) ion in sites of tetrahedral symmetry have been detected directly by far-infrared optical absorption in crystals of cubic  $\text{ZnS}$ <sup>1</sup> and CdTe,<sup>2</sup> in the range below  $100 \text{ cm}^{-1}$ . For ZnS the number, position, and intensities of the absorption peaks at  $4^\circ\text{K}$  can be accounted for by simple crystal-field theory in terms of the spin-orbit splitting of the  ${}^5E$  ground state.<sup>1,2</sup> In CdTe, however, the  $\text{Fe}^{2+}$  spectrum does not fit this theory and in particular exhibits additional lines.<sup>2</sup> The purpose of this paper is to consider a model which can account for this spectrum by augmenting crystal-field theory to include dynamic Jahn-Teller coupling between the  ${}^5E$  state of the  $\text{Fe}^{2+}$  ion and a low-frequency vibrational mode of the CdTe lattice.

The crystal lattices of cubic  $\text{ZnS}$ <sup>3</sup> and CdTe,<sup>4</sup> in common with other II-VI compounds, have the transverse acoustic (TA) branch of the phonon spectrum at a quite low frequency. For cubic ZnS, however, the critical points in this branch are above the energies of the excited levels of the  $\text{Fe}^{2+}$  ion to which the far-infrared transitions take place. The Jahn-

Teller coupling of the  ${}^5E$  state of the  $\text{Fe}^{2+}$  ion to these and other vibrational modes is apparently weak,<sup>1</sup> and no definite evidence of a Jahn-Teller effect in the  ${}^5E$  state of  $\text{ZnS:Fe}^{2+}$  has been found. For CdTe, on the other hand, the critical points in the TA branch are so low as to lie among these  $\text{Fe}^{2+}$  levels. Some of these phonons moreover have the correct symmetry to participate in Jahn-Teller coupling with the  ${}^5E$  state of the substitutional  $\text{Fe}^{2+}$  ion. As we will show, such a coupling, though weak, nevertheless can appreciably distort the electronic absorption spectrum and can introduce extra lines as found experimentally.

In addition to those phonons which contribute to the Jahn-Teller coupling, other lattice phonons from the TA branch may be optically excited as a result of the electron-phonon coupling with the  $\text{Fe}^{2+}$  ion, and these may contribute additional structure as sidebands to the lines of the electronic absorption spectrum. We will see that there is also evidence for extra absorption of this sort in the experimental spectrum.

In this paper we first review briefly in Sec. II the relevant predictions of crystal-field theory for the  $\text{Fe}^{2+}$  ion,<sup>1,5</sup> including the effect of spin-spin in-